Superconductor Science and Technology

PAPER • **OPEN ACCESS**

Advanced experimental-based data-driven model for the electromechanical behavior of twisted YBCO tapes considering thermomagnetic constraints

To cite this article: Mohammad Yazdani-Asrami *et al* 2022 *Supercond. Sci. Technol.* **35** 054004

OPEN ACCESS
IOP Publishing

Superconductor Science and Technology

Supercond. Sci. Technol. **35** (2022) 054004 (13pp)

https://doi.org/10.1088/1361-6668/ac57be

Advanced experimental-based data-driven model for the electromechanical behavior of twisted YBCO tapes considering thermomagnetic constraints

Mohammad Yazdani-Asrami[1,*], Alireza Sadeghi[2], Seyyed Meysam Seyyedbarzegar[2] and Amirhossein Saadat[2]

[1] James Watt School of Engineering, University of Glasgow, Glasgow, United Kingdom
[2] Department of Electrical Engineering, Shahrood University of Technology, Shahrood, Iran

E-mail: mohammad.yazdani-asrami@glasgow.ac.uk

Received 24 October 2021, revised 27 January 2022
Accepted for publication 21 February 2022
Published 4 April 2022

Abstract

Data-driven models can predict, estimate, and monitor any highly nonlinear and multi-variable behaviour of high-temperature superconducting (HTS) materials, and superconducting devices to analyse their characteristics with a very high accuracy in an almost real-time procedure, which is a significant figure of merit as compared with traditional numerical approaches. The electromechanical behaviour of twisted HTS tapes under different strains, magnetic fields, and temperatures is a complicated problem to be solved using conventional approaches, including finite element-based methods, otherwise, experimental testing is needed to characterise it. This paper aims to offer a data-driven model based on artificial intelligence techniques to predict the electromechanical behaviour of HTS tapes operating under various thermomagnetic conditions. By using the proposed model, normalised critical current value and stress of twisted tapes can be predicted under different temperatures and magnetic flux densities. For this purpose, experimental data were used as inputs to design an adaptive neuro-fuzzy inference system (ANFIS). To achieve the best performance of the prediction system, multiple clustering methods were used, such as the grid partitioning method, fuzzy c-means clustering method, and sub-clustering method. Sensitivity analyses were conducted to find the best architecture of ANFIS to predict and model electromechanical behaviour of twisted tapes with high accuracy.

Keywords: artificial intelligence, critical current density, data-driven model, mechanical stability, strain, stress, twisting

(Some figures may appear in colour only in the online journal)

* Author to whom any correspondence should be addressed.

1. Introduction

The discovery of high-temperature superconducting (HTS) materials was the origination of many investigations to take advantage of superconductors in engineering fields including large-scale power applications [1, 2]. These materials in the form of coated conductors are employed to fabricate superconducting cables [3, 4], superconducting transformers [5, 6], superconducting fault current limiters [7, 8], superconducting busbars, and many other high-power electric devices in power grids. In addition, another promising and fast-growing application of HTS materials is in cryo-electrifications of modern transportation systems such as electric aircraft [9] and marine applications [10]. In many power applications, tapes are usually twisted around a former to minimise AC loss. Twisting imposes mechanical tension to the HTS tapes and causes a critical current reduction [11]. This mechanical tension could damage the brittle superconducting layer, and as a result, generate weak points along the length of HTS tapes in such a way that even during normal operation, this could lead to malfunction or to complete failure of HTS device.

The characterisation of the critical currents and the applied mechanical stresses of twisted superconducting tapes is an electromagnetic coupled with thermomechanical problem. To solve this, there are analytical methods with low accuracy and difficulties for dealing with complicated geometries. To address these issues, finite element method (FEM) was proposed. Although FEM-based approaches have higher accuracy, their computation time and cost are extremely high. The high computation burden makes FEM-based approaches inappropriate for applications that require a fast computation response (FCR) or real-time response (RTR). One may propose experimental analyses for solving the aforementioned problem [12–14]. These methods are more accurate and faster than previous methods, i.e., analytical and FEM-based methods. However, sometimes the time spent preparing and developing an experimental set-up is considerable. Moreover, in FCR and RTR systems, especially those implemented in cryo-electrified aircraft or other transportation units, there is no time/room for tests and superconducting tapes have to operate just right, considering safety concerns. So, artificial intelligence (AI) techniques can be developed and used as a solution to the aforementioned problems with acceptable accuracy and very low computation time. AI-based methods can be implemented in applications with a requirement for FCR or RTR systems to estimate the behaviour of any kind of HTS tape [15]. For instance, and in the coming future, by developing an accurate surrogate model using AI techniques, the electro-magneto-thermo-mechanical properties of HTS tapes/devices would be estimated in a few milliseconds while the HTS device is operating in any cryo-electrified transportation system.

In this paper, a data-driven model based on the adaptive neuro-fuzzy inference system (ANFIS) is proposed to estimate the electromechanical characteristic of Second generation (2G) HTS tapes as an intelligent package with an easily implementable structure, very high accuracy, and ultra-high estimation speed. The proposed method can characterise the electromechanical behaviour of HTS tapes with respect to thermomagnetic considerations. So, the inputs of the critical current estimation are width, thickness, magnetic flux density, temperature, and strain value (ϵ) and the output is the minimum critical current of tape. For the estimation of the stress, inputs are reduced to four. This is because of the independency of the stress from the magnetic flux density. In this paper, electromechanical behaviour of multiple Yttrium Barium Copper Oxide (YBCO) tapes (produced by different manufacturers) is estimated by ANFIS in MATLAB software package using experimental results as input data.

2. Electromechanical behaviour of HTS tapes subjected to twisting

The AC loss in the superconducting tapes could be affected and intensified by many factors, namely temperature increase [16], harmonic distortions [17], level of carrying current, frequency change, level of external magnetic field, among others. The poor dissipation of AC loss leads to heat accumulation, and consequently temperature increase of HTS tapes, as well as efficiency reduction of the cooling unit and the whole device [18]. As a way to overcome this problem, tapes are wounded on the former to reduce the AC loss and diminish the temperature rise. It should be noted that the concept of twisting is usually used in HTS cables, and magnets. Figure 1(a) presents a twisted tape and two important twisting parameters, pitch angle and pitch length. Twisting pitch length (TPL) is defined as the length within which an HTS tape gets back to its initial relative position and the twisting pitch angle (TPA) is defined by equation (1) [19]:

$$\alpha = \tan^{-1}\frac{\ell}{2\pi R} \tag{1}$$

where ℓ is TPL and R is the radius of the former on which the HTS tape is twisted.

Twisting causes a specific type of deformation in HTS tape, known as strain. As a matter of fact, strain is the displacement between the particles in the body of the HTS tape relative to its length [12]. When twisting applies a pure torsional load to the HTS tape, the value of the strain is not constant on the surface of HTS tapes. In fact, the strain is distributed non-uniformly at different locations of tape. So, strain is a function of the location of the calculation point, TPA, TPL, temperature, and the structure of the HTS tape [12]. The reduction of critical current and the increase of mechanical stress are the consequences of twisting of the tapes around a former and the resulted strain. Thus, AC loss would be reduced but this advantage is achieved at the cost of generating some weak points on HTS tapes, if twisting is not applied under proper tension and angle. These weak points have a lower critical current than the expected value, locally. So, more heat would be generated in these points, which causes a significant temperature increase, making these points a good candidate for establishing hotspots. In fact, if TPA surpasses a specific value, HTS tapes experience a significant reduction in critical current and

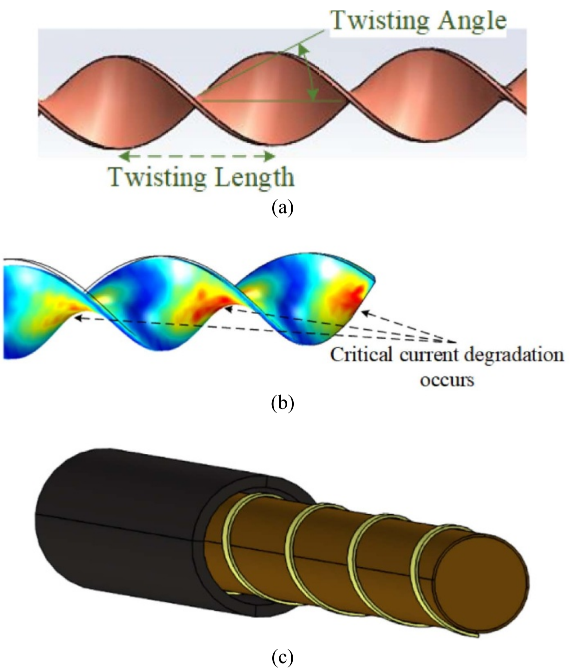

Figure 1. The concept of twisting pitch in HTS tapes and cables. (a) The definition of TPA and TPL (b) possible points of critical current degradation (c) a schematic of twisting on a single layer HTS cable.

may even cause thermomagnetic collapse of the tapes. Another impact of twisting is the applied mechanical stress on the tape which is a function of the strain. Possible locations for critical current degradation along the length of superconducting tape are shown in figure 1(b). A simple schematic of a twisted HTS tape in a superconducting cable is also shown in figure 1(c).

3. The proposed ANFIS methodology

ANFIS is a highly accurate estimation and prediction AI-based method that operates as a first-order Takagi-Sugeno-Kang (TSK) fuzzy system. In fact, a fuzzy interference system is combined with adaptive neurons to create a structure for prediction and estimation known as ANFIS. Firstly, ANFIS obtains a group of data as train inputs and outputs. In this stage, ANFIS uses learning rules such as back propagation, gradient descent, and the least square method to map the inputs to the outputs. After gaining a proper structure for the problem, test inputs are inserted to prove the capability of the model in predicting the test outputs. The objective is to reduce the error function to the lowest possible value [20–22] i.e. minimize it. This procedure is shown in figure 2 for a general structure of ANFIS with one input and output that tends to reduce the error. For this purpose, the mean square error (MSE) index is defined by equation (2):

$$\mathrm{MSE} = \frac{1}{N}\sum_{i=1}^{N} e_i^2 = \frac{1}{N}(t_i - y_i)^2 \tag{2}$$

where, N is the number of training data, e_i is the difference between each real value and its estimated value, t_i is the targets and y_i is the output of the TSK fuzzy system.

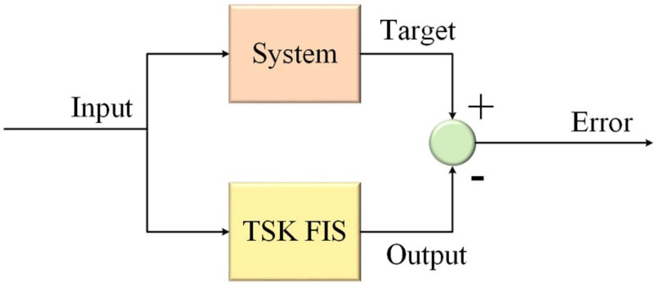

Figure 2. A general structure of an ANFIS.

The relation between input (x_i) and output (y_i) of the fuzzy system is defined by equation (3):

$$y_i = \frac{\sum_{l=1}^{M} y^{-l} \prod_{i=1}^{N} e^{-\left(\frac{x_i - m_i^l}{\sigma_i^l}\right)^2}}{\sum_{l=1}^{M} \prod_{i=1}^{N} e^{-\left(\frac{x_i - m_i^l}{\sigma_i^l}\right)^2}} \tag{3}$$

where, m_i^1, σ_i^l are parameters of Gaussian membership functions that are regulated by the gradient descent method to minimize the MSE [23, 24]

$$m_i^l(k+1) = m_i^l(k) - \alpha\frac{\partial e}{\partial m_i^l}. \tag{4}$$

$$\sigma_i^l(k+1) = \sigma_i^l(k) - \alpha\frac{\partial e}{\partial \sigma_i^l} \tag{5}$$

where, k is number of iterations and α is tune coefficient.

There are three different methods to generate a preliminary fuzzy system which are discussed in the following subsections.

3.1. *Grid partition method (GPM)*

The GPM operates based on the creation of fuzzy rules from numerical pairs. The minimum and the maximum of each input vector are calculated according to equation (6) and their differences are classified with respect to membership functions [25]:

$$\begin{cases} x_i^{\min} = \min\limits_p x_i(p) \\ x_i^{\max} = \max\limits_p x_i(p) \end{cases}, x_i(p) \in \left[x_i^{\min}, x_i^{\max}\right], \quad p = 1, 2, \ldots, p, i = 1, .., N. \tag{6}$$

At the final step with respect to the input vector and membership functions, the inputs domain is partitioned. Then, the fuzzy rules of the TSK fuzzy system are written based on input data as equation (7) [25]:

$$R^j: \text{ if } x_1 \text{ is } A_1^j \text{ and} \ldots \text{and } x_n \; is \; A_n^j \text{ then } y = f(x_1, \ldots, x_N) \tag{7}$$

where, R^j is the jth fuzzy rule and A_N^j is the jth linguistic variable for Nth input.

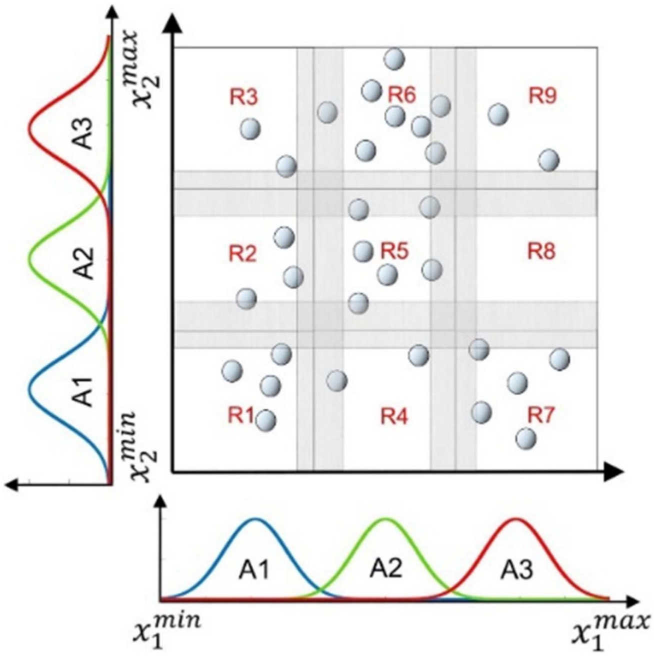

Figure 3. Schematic of grid partition clustering method.

A schematic of the GPM clustering method is shown in figure 3. As shown in this figure, by dividing the input vector into many fuzzy parts, GPM generates partitions.

3.2. Fuzzy C-means clustering method (FCM)

In FCM, every data point belongs to multiple clusters with different membership orders. The FCM performs based on minimizing the objective function of equation (8) [26, 27]:

$$J_m = \sum_{i=1}^{N} \sum_{j=1}^{N_C} \mu_{ij}^m \|x_i - c_j\|^2 \tag{8}$$

where, N_C is the number of clusters, c_j is the centre of jth cluster and μ_{ij}^m is the membership degree of x_i to the membership function of jth cluster, and m is fuzzy separation matrix.

All cluster centres are updated with equation (9):

$$c_j = \frac{\sum_{i=1}^{N} \mu_{ij}^m x_i}{\sum_{i=1}^{N} \mu_{ij}^m}. \tag{9}$$

The value of μ_{ij} is also obtained from equation (10):

$$\mu_{ij} = \frac{1}{\sum_{h=1}^{N} \left(\frac{\|x_i - c_j\|}{\|x_i - c_h\|} \right)^{\frac{2}{m-1}}}, \quad 0 \le \mu_{ij} \le 1, \quad m > 1 \tag{10}$$

where m determines the fuzzy degree of the borders between clusters. Updating cluster centres with equation (9) and determining the data membership degree in each cluster with equation (10) is repeated until centres of clusters do not have a tangible change. Figure 4 represents the FCM method as another option in clustering.

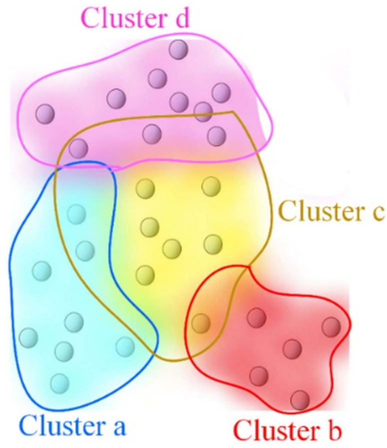

Figure 4. Schematic of fuzzy c-mean clustering method.

3.3. Subtractive clustering method (SCM)

In the SCM, it is assumed that all data could be the centre of the cluster and the score of each point as a centre is calculated. The influence of clustering in the problem space is determined by radius (r) and for each point, the mean distance to all points in the radius of that point is considered as a factor for scoring. In the end, the best centre of the cluster is selected based on the score points. The score of each point is calculated by equation (11) [28]:

$$\sigma_i = \sum_{j=0}^{n} \exp\left(-\frac{\|x_i - x_j{}^2\|}{\left(\frac{r}{2}\right)^2} \right). \tag{11}$$

Based on the considered radius of influence, the data that are dominated by the cluster centre are removed. Then for the remaining data, another cluster centre is selected, and this continues until the end of all data clustering. The data membership degree in each cluster is determined by equation (12):

$$\mu_{ij} = \exp\left(-\frac{1}{2} (x_i - c_j)^{\mathrm{T}} \Sigma^{-1} (x_i - c_j) \right) \tag{12}$$

where c_j is the cluster centre defined by equation (13):

$$\Sigma = \begin{bmatrix} 1 & & 0 \\ & \ddots & \\ 0 & & \sigma_N \end{bmatrix}. \tag{13}$$

This clustering method is depicted in figure 5.

3.4. General remarks on GPM, SCM, and FCM

In GPM, fuzzy rules are designed for all cases which may never be used during the estimation and increase the computation cost. While in clustering techniques, the number of fuzzy rules significantly decreases. Instead of writing fuzzy rules for each of the data that causes complexity, a fuzzy rule is considered for each cluster that simplifies the calculations. In SCM, unlike FCM, the number of clusters cannot be directly specified. But by changing the radius of influence, a control the

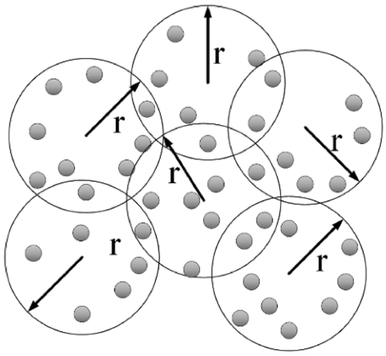

Figure 5. Schematic of subtractive clustering method.

number of clusters can be achieved. However, determining a small radius of influence usually produces more clusters and more fuzzy rules.

4. Results and discussions

The ANFIS—similar to any other data-driven method—requires some input data. In this paper, results of experimental tests were used as input data to ANFIS. In [29–37], the experimental data are attained with respect to the electromechanical behaviour of different YBCO tapes under various thermo-magnetic conditions based on the procedure shown in figure 6. The first step is to apply a mechanical load to the coated conductor. Step-motors are normally used to apply mechanical loads. These loads cause mechanical stresses on tape which results in the critical current reduction and imposing stress to the tape. Stress can be measured by an extensometer. The value of critical current can be measured by measuring the current and voltage, and temperature [38]. Table 1 tabulates the specifications of the selected HTS tapes.

To create a model based on ANFIS, data were gathered under various temperatures, fields, and strains. The aforementioned gathering data phase is depicted as the experimental data acquisition phase in figure 7. About 50% of these data (total number of 125) was chosen randomly (to eliminate any chance of being biased to any specific data) to use in the training phase as inputs and outputs. At this level, the model is trained to characterise the electromechanical behaviour of YBCO tapes. After reaching the minimum error function, the model proceeds to the next phase. In this phase, the established model obtains some input data as test inputs. The test inputs are those which have remained from the random selection process, i.e., the other 50% of the experimental data (125 data points). This means that neither of the test inputs is the same as the training inputs. In other words, the ANFIS never saw the test data during the training phase. This is shown to be the test phase in figure 7. Finally, the system estimates the test outputs with respect to the laws, rules, and clusters gained from the training phase of the modelling system.

It should be noted that, for the sake of comparison among different methods, root mean square error (RMSE) and correlation coefficient (R^2) are analysed as the most famous and common error criteria, which are expressed in equations (14) and (15). RMSE is usually used to show the difference between an estimated value and real data while the correlation coefficient is a statistical quantity that shows the strength of the correlation between the real values and predicted ones:

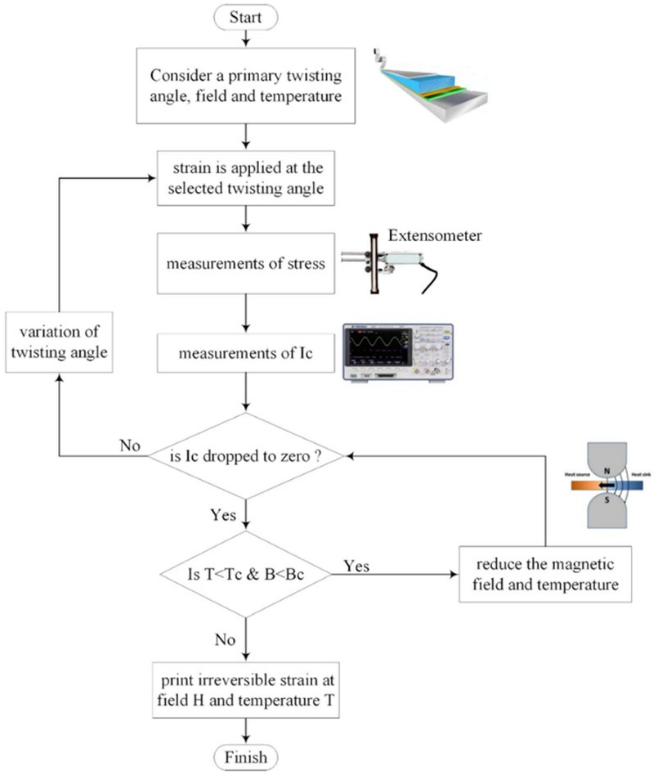

Figure 6. The procedure of measuring critical current/stress of YBCO tapes in [29–37].

$$\mathrm{RMSE} = \sqrt{\sum_{k=1}^{N} \frac{(A_k - F_k)^2}{N}} \tag{14}$$

$$R^2 = \frac{\sum_{k=1}^{N} (A_k - \bar{A})(F_k - \bar{F})}{\sqrt{\sum_{k=1}^{N} (A_k - \bar{A})^2 \sum_{k=1}^{N} (F_k - \bar{F})^2}} \tag{15}$$

where N is the number of data, A_k is the value of real experimental data, F_k is the value of the forecasted data, $\bar{A}$ is the mean of experimental data, and $\bar{F}$ is the mean of forecasted data.

4.1. Smart estimation of critical currents (I_c)

Figure 8 presents the estimated values of the normalized critical current with respect to variations of strain, magnetic flux density, and temperature by ANFIS for different tapes. It is worth noting that the value of the magnetic flux density is 19 T at 4.2 K and the self-field (no external magnetic flux density) at 77 K. Figure 8 is produced based on three mentioned clustering methods, namely FCM, GPM, and SCM. To plot figure 8, the

Table 1. Specifications of superconducting tapes used for analysing data [29–37].

Tape manufacturer	Width (mm)–thickness (μm)	Technology	Substrate-type of Cu stabilizer
SuperPower—tape a	4.19–115	IBAD/MOCVD	Hastelloy-electroplated
SuperPower—tape b	4–101	IBAD/MOCVD	Hastelloy-electroplated
SuNam	4–110	IBAD/RCE	Hastelloy-electroplated
Bruker HST	4.1–153	ABAD/PLD	Stainless steel-electroplated
Fujikura	3.05–161	IBAD/PLD	Hastelloy-laminated
SuperOx	4.04–112	IBAD/PLD	Hastelloy-electroplated

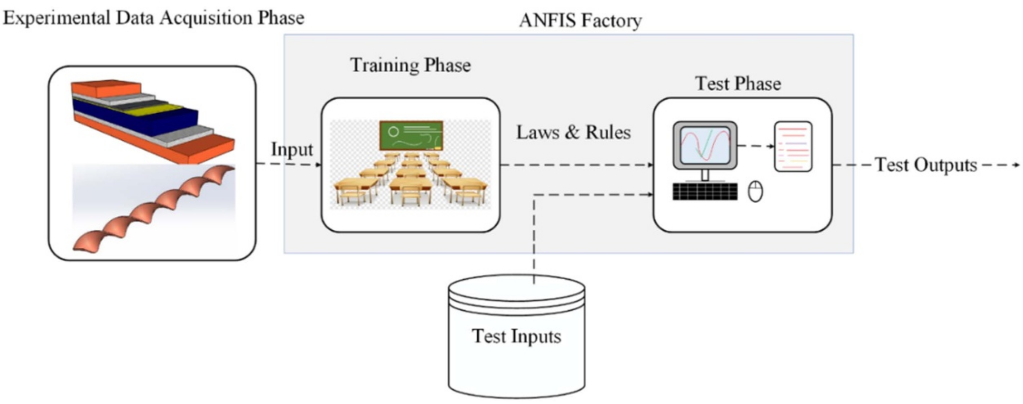

Figure 7. The procedure of estimation by ANFIS.

fastest clustering methods among FCM, SCM, and GPM are chosen. A comprehensive sensitivity analysis on ANFIS parameters were done and results were listed in table 2. Table 2 summarises the values of RMSE, computation time, and correlation coefficient (R^2) for different clustering methods. It is worth noting that the computation time depends on the configuration of the computer that is used for computing; in our case, the specification of the computing system is as follows: RAM: 16 GB-DDR3, CPU: Corei7-3612QM-2.1 GH. It is worth noting that all computations were done using same computer for all different methods; therefore, the relative difference between them from the computation time viewpoint is still valid.

Speed of estimation or computation time is a crucial factor for applications that require a fast prediction of the characteristics of HTS tapes. On the other hand, accuracy is another vital factor to appropriately characterise the electromechanical behaviour of HTS tapes. Among all clustering methods, FCM3 with three membership functions has the highest estimation speed. For the sake of more assessments, the FCM with six (FCM6) and nine (FCM9) membership functions were tested, as well. By doing this, it is found that the computation time of FCM6 and FCM9 compared with FCM3 is 76.6% and 150.5% increased, respectively. Also, for more investigation, FCM3 was compared with respect to GPM and SCM. In comparison to the fastest GPM and SCM, FCM3 has a 1062% and 22.1% higher estimation speed, respectively. Thus, for FCR or RTR systems, GPM is completely out of list due to low speed or high computation time.

Considering the accuracy of the estimations, sub-clustering with a radius of 0.5 (SCM0.5) has the lowest RMSE and highest R^2. The SCM was also investigated with different clustering radii of 0.1 (SCM0.1) and 1 (SCM1). The results show that the accuracy of the SCM was reduced by 20% using SCM0.1 and by 93.5% using SCM1 compared to SCM0.5. Therefore, SCM0.5 is recommended for achieving highest possible accuracy with SCM.

Another factor that can be effective in choosing the appropriate ANFIS method is to consider accuracy and speed simultaneously. However, in some applications some levels of trade-off between estimation accuracy and speed maybe needed. Analysing the results of the best accuracy with the highest speed shows that although FCM3 has a 360% higher speed than SCM0.5, the RMSE value of SCM0.5 is 40.51% lower and R^2 is 25.91% higher than FCM3. Therefore, if one considers the speed and accuracy simultaneously, more discussions are needed on different considerations. In accordance with this approach, figure 9 illustrates the different aspects of choosing a clustering method and it shows which of these methods can fulfil the speed and accuracy considerations.

As shown in figure 9, the methods which lay in the green zone are selected as the fastest methods while the methods in the purple zone have the highest accuracy. If one just considers the estimation speed, the fastest results are extracted from FCM3, SCM1, FCM6, and FCM9, respectively, while the methods with the highest accuracy are SCM0.5, GPM1, SCM0.1, and FCM9, respectively. The overlap of these two zones is FCM9 with RMSE of 0.0579, and R^2 of 0.811. FCM9 has 150% higher computation time than FCM3 and 23% higher RMSE than SCM0.5. So, FCM9 is as the best method of clustering when I_c is

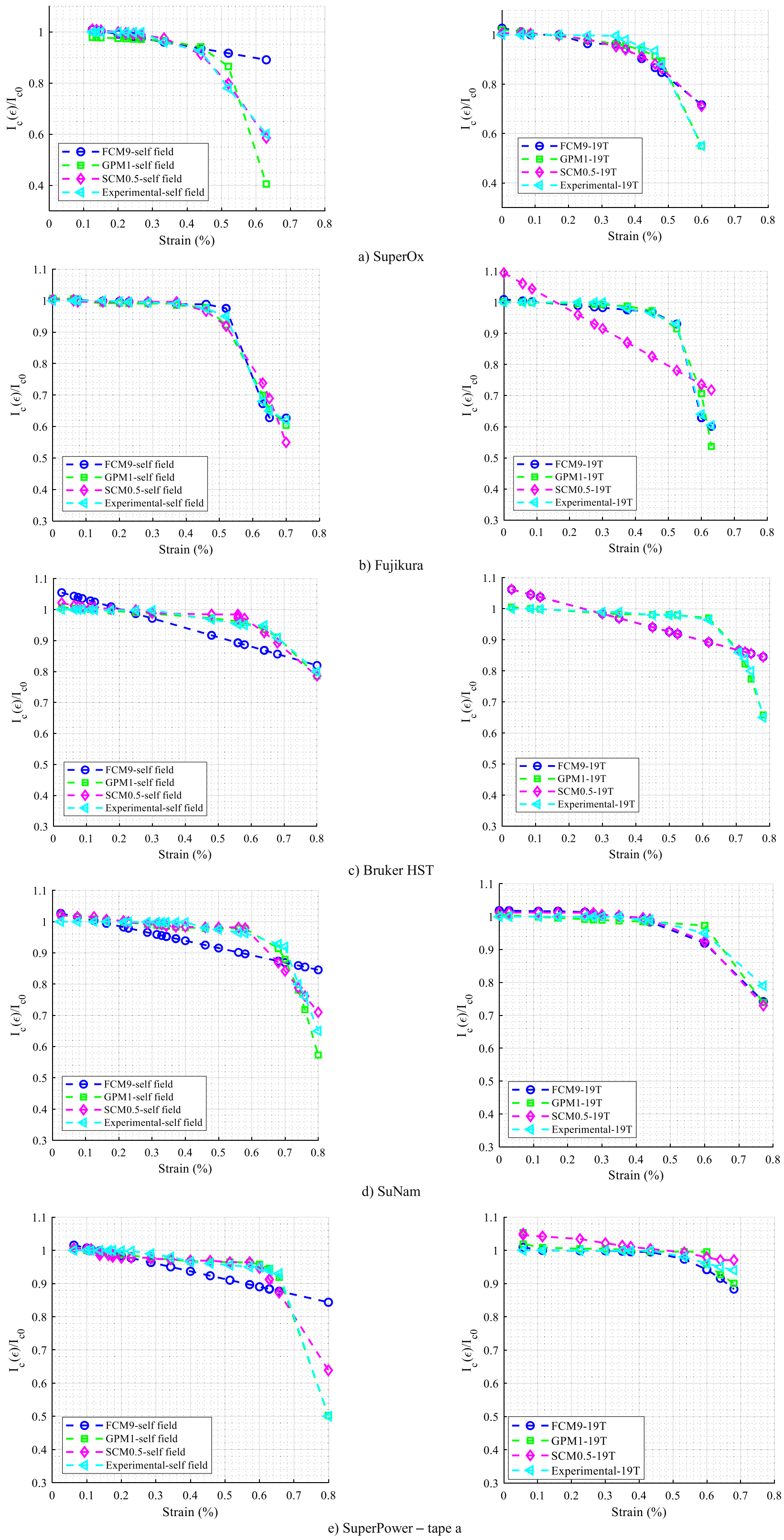

Figure 8. Estimation of the normalised critical currents versus different strain (∈) with respect to their magnetic flux density and temperature.

Table 2. Comparison of the accuracy and the computation time of different clustering methods of ANFIS for estimating normalised critical current.

Method	FCM3	FCM6	FCM9	GPM1	GPM2	GPM3	SCM0.1	SCM0.5	SCM1
Computation time (s)	0.628	1.109	**1.573**	**7.298**	42 876.797	138 063.286	8.821	**2.886**	0.767
RMSE	0.066	0.071	**0.057**	**0.05**	0.367	0.151	0.056	**0.047**	0091
R^2	0.731	0.709	**0.811**	**0.914**	0.75	0.77	0.814	**0.92**	0.657

The bold values show the best performance of a scenario of a clustering method, when compare it to other scenarios of the same clustering method.

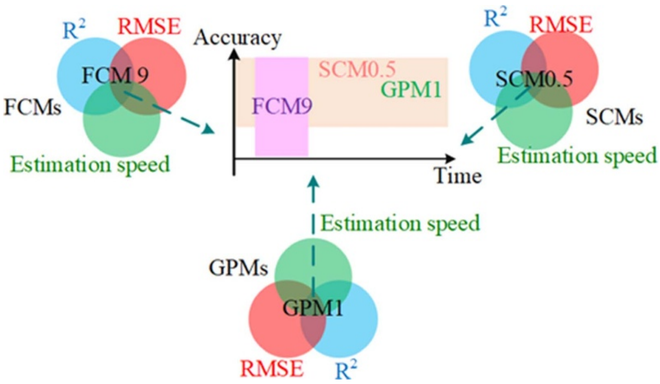

Figure 9. Venn diagram of the most accurate and the fastest methods to estimate the critical current.

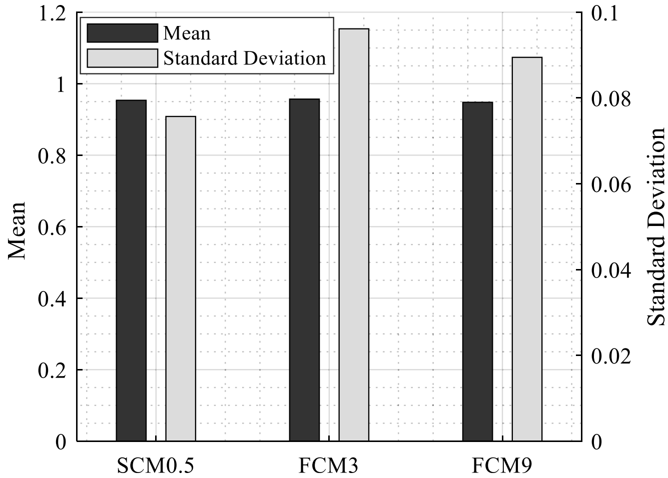

Figure 11. Mean and standard deviation comparison of three ANFIS methods for critical current estimation.

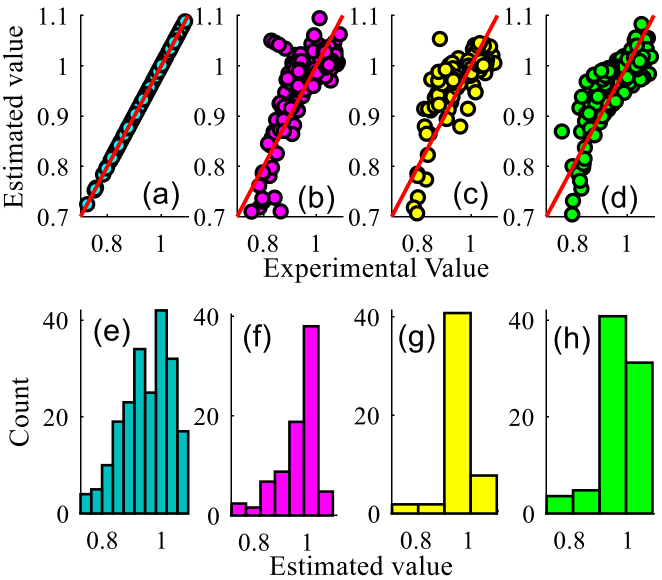

Figure 10. Comparison the results of experimental values (a)–(e) with estimated values namely, SCM0.5 (b)–(f), FCM3 (c)–(g), and FCM9 (d)–(h), (a)–(d) plot of estimated value against experimental data, (e)–(h) histogram plot of data for different types of clustering and experimental.

estimated concerning simultaneous effect of accuracy and speed.

Figures 10(a)–(d) plots the values of the estimated critical current by ANFIS versus the experimental values for all tapes. This figure shows how estimated values are well-matched with experimental data which were used as input to ANFIS system. In figure 10(a), the figure is plotted for the experimental versus the experimental which should technically give us the $y = x$ line. This figure is an index for analysing the proper performance of three methods which were discussed before against the experimental results. The first method is SCM0.5 with the highest accuracy among all other methods which shows a very similar characteristic to the pattern of experimental results. After that FCM3 is depicted by yellow colour with the highest speed of estimation. As it can be observed, figure 10(a) has the lowest similarity to the first figure, i.e. experimental results pattern. At last, there is the chosen method that meets both speed and accuracy. Figures 10(e)–(h) represents the histogram plot of data in different clustering methods. The subplot with more similar behaviour to figure 10(e) has higher accuracy (i.e. SCM0.5). Figure 11 shows the mean and standard deviation of predicted data for three different ANFIS methods. The mean of the estimated values of the three clustering methods are very close to each other while SCM0.5 has the lowest standard deviation due to its high accuracy; after that there are FCM9 and FCM3, respectively.

4.2. *Smart estimation of stress*

Temperature and strain are two important parameters that can change the stress on HTS tapes. Figure 12 depicts the values of estimated stresses and compares them with the experimental values. These values are estimated for different types of tapes with different clustering methods. It is worth noting that data were reported in two temperatures, i.e. 4.2 K and 77 K. For stress estimation, FCM3, GPM1, and SCM0.1 are the most

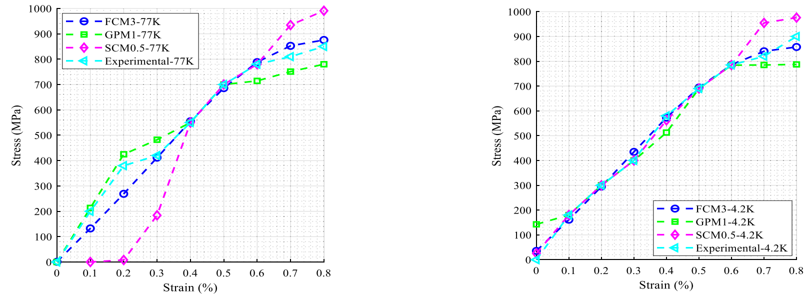

a) SuperPower- Tape a

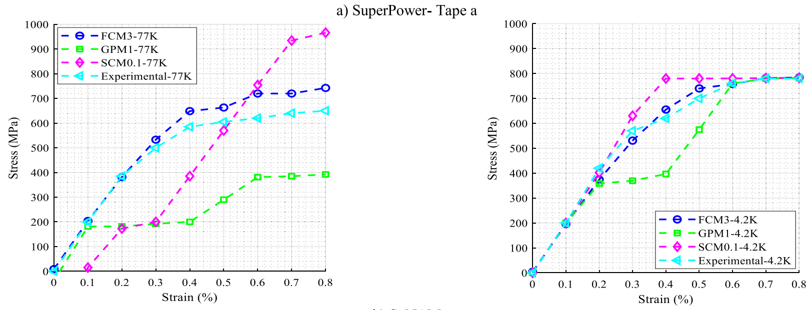

b) SuNAM

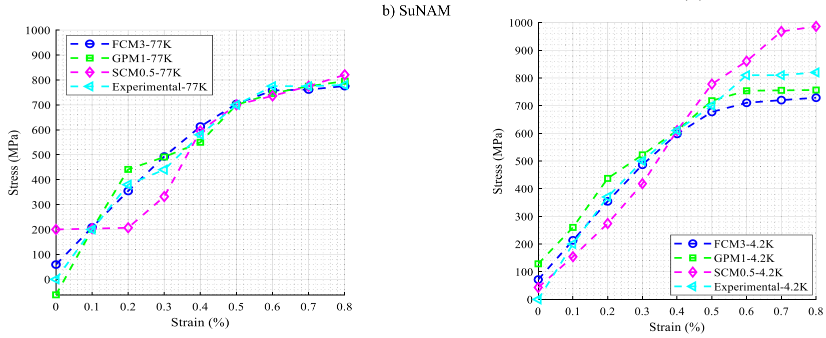

c) SuperPower- Tape b

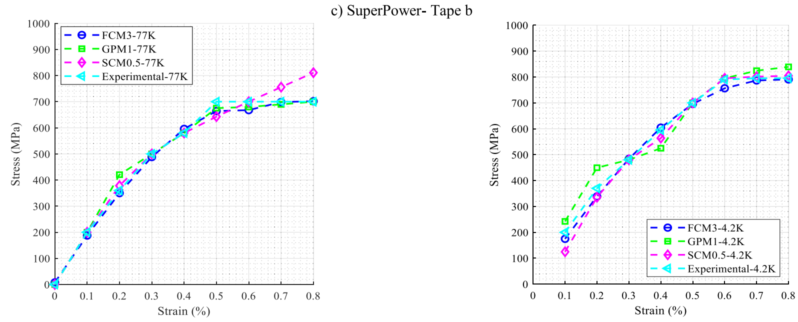

d) Bruker HST

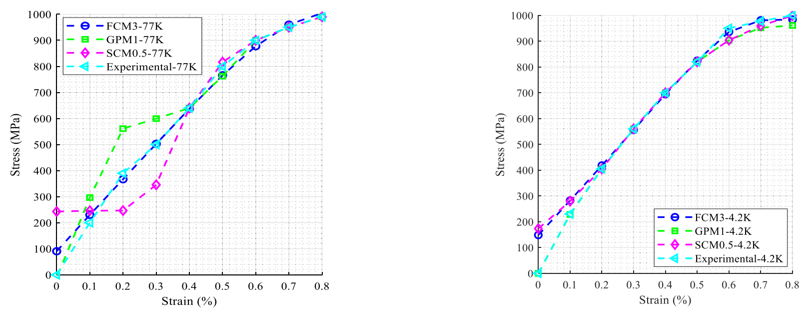

e) SuperOx

Figure 12. Stress prediction of HTS tapes versus strain ($\in$) with respect to the temperature.

Table 3. Comparison of the accuracy and the computation time of different clustering methods of ANFIS for estimating stress in 2 G HTS tapes.

Method	FCM3	FCM6	FCM9	GPM1	GPM2	GPM3	SCM0.1	SCM0.5	SCM1
Computation time (s)	**0.780**	0.802	0.936	**8.001**	615.189	2039.285	**6.594**	2.537	0.689
RMSE	**41.988**	167.596	216.664	**126.943**	165.203	2076.208	**110.139**	175.983	213.311
R^2	**0.989**	0.892	0.788	**0.914**	0.881	0.883	**0.938**	0.855	0.775

The bold values show the best performance of a scenario of a clustering method, when compare it to other scenarios of the same clustering method.

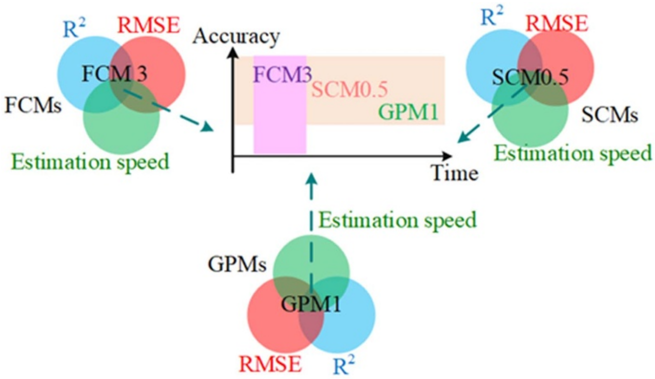

Figure 13. Venn diagram of the most accurate methods and the fastest methods to estimate the stress.

accurate clustering methods which are used to plot the data in figure 12.

The computation time, RMSE, and R^2 indices are tabulated in table 3 for the stress estimation process. According to table 3, the fastest method is SCM1 with a speed between 1x-11667x faster than other methods while the most accurate method based on R^2 is FCM3 with an R^2 between 5.5% and 27.6% higher than other approaches. If speed is considered for selecting a method, GPMs are completely out of list. However, if both speed and accuracy are considered together, according to figure 13, two categories of solutions can be formed. SCM1, FCM3, FCM6, and FCM9 are the fastest methods, respectively and FCM3, SCM0.1, GPM1, and FCM6 have the highest accuracy, respectively. Accordingly with respect to table 3 and figure 13, it can be stated that FCM3 has the highest trade-off of speed and accuracy, simultaneously. Therefore, FCM3 is the best clustering method for the estimation of the stress characteristic in YBCO tapes.

Figure 14 compares the methods which meet the speed and the accuracy constraints. Figure 14(a) is plotted for experimental versus experimental data (it perfectly lies on $y = x$ linear line), while the vertical axis in figures 14(b) and (c) is the estimated values. As it can be seen from figure 14(b), the FCM3 has a more similar characteristic and pattern to the figure 14(a). The same comparison is valid for figures 14(d)–(f). For figures 14(d)–(f), it should be mentioned that the distribution of the data does not necessarily need to be normal distribution and the data with more similar behaviour to the figure 14(d) has the highest accuracy. Figure 15 also compares the value of mean and standard deviation of estimated values for FCM3 and SCM1 methods. FCM3 has a lower standard deviation and therefore, higher accuracy in comparison to SCM1.

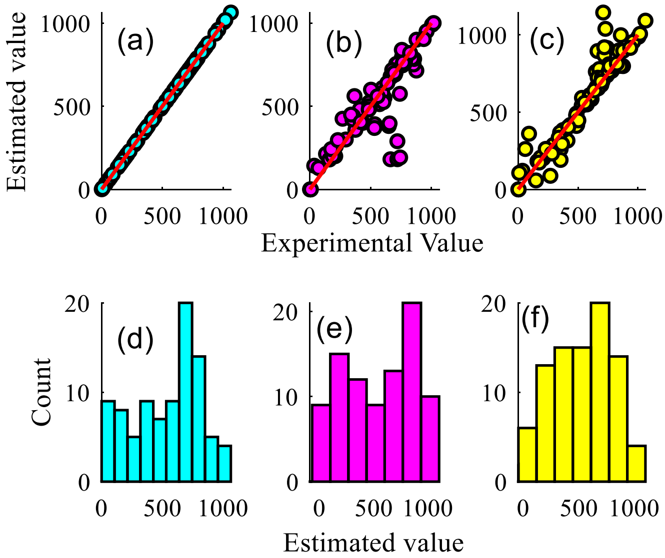

Figure 14. Comparison the results of experimental values (a)–(d) with estimated values namely, SCM1 (b)–(d) and FCM3 (c)–(f), (a)–(c) plot of estimated value against experimental data, (d)–(f) histogram plot of data for different types of clustering and experimental.

5. Verification of model

In general, this section is provided to show the effectiveness and capability of the proposed model in estimating the values of critical current versus the magnetic flux density out of the training bound. By the capability of the model to accurately estimate the electromechanical characteristic, a real-time implementation of such model in near future would be possible, given the fact that high performance computational resources will be more accessible soon. To do this, the SuperPower-tape b is selected and magnetic flux density of 0, 0.1, 0.3, 0.5, 1, 2, 3 T are applied, which was not among any of the previous data sets. Figure 16 presents the estimated values for different clustering methods. This is also simulated by FCM9, GPM1, and SCM0.5. The values of RMSE and R^2 of the model verification for all clustering methods are tabulated in table 4. According to table 4, again FCM9 could be chosen as the method which satisfies both time and the accuracy constraints. The R^2 value of

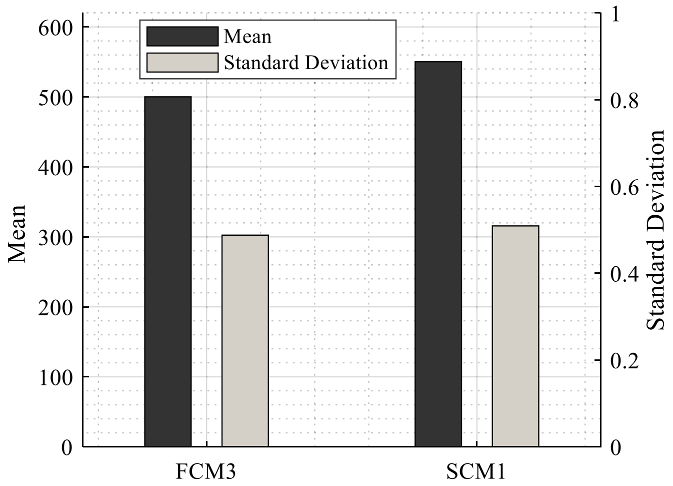

Figure 15. Mean and standard deviation comparison for two methods of stress estimation.

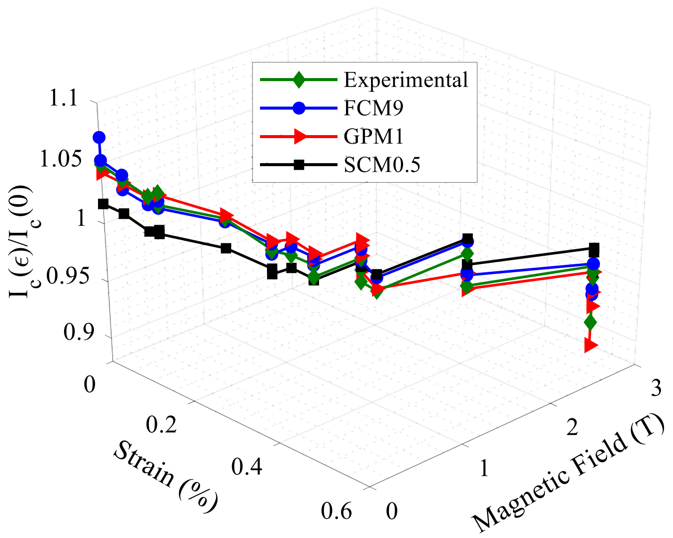

Figure 16. Model validation of ANFIS for HTS tape of superpower—tape b.

Table 4. Error evaluation for the model verification process for HTS tape of superpower—tape b.

Method	FCM3	FCM6	FCM9	GPM1	GPM2	GPM3	SCM0.1	SCM0.5	SCM1
Computation Time (s)	0.153	0.611	**0.745**	**2.301**	111.966	668.196	3.905	**1.346**	0.194
RMSE	0.051	0.062	**0.032**	**0.022**	0.311	0.197	0.024	**0.019**	0.088
R^2	0.801	0.788	**0.887**	**0.922**	0.701	0.78	0.751	**0.951**	0.681

The bold values show the best performance of a scenario of a clustering method, when compare it to other scenarios of the same clustering method.

FCM9 is 16% higher than FCM3, as the fastest method, and computation time of the FCM9 is 45% lower than SCM0.5, as the most accurate method. Thus, it must be claimed that the FCM9 is the best choice for the critical current estimation. The structure of the FCM9 is shown in figure 17(a) in which for every input, nine membership functions are considered. They are tape thickness, tape width, strain, magnetic flux density, and temperature. Figure 17(b) presents the range of variations for each input whereas the membership functions gain a value between 0 and 1, known as membership degree. The summation of membership degrees for each input must be equal to 1. Different membership functions are related to each other by fuzzy rules to identify the value of inputs.

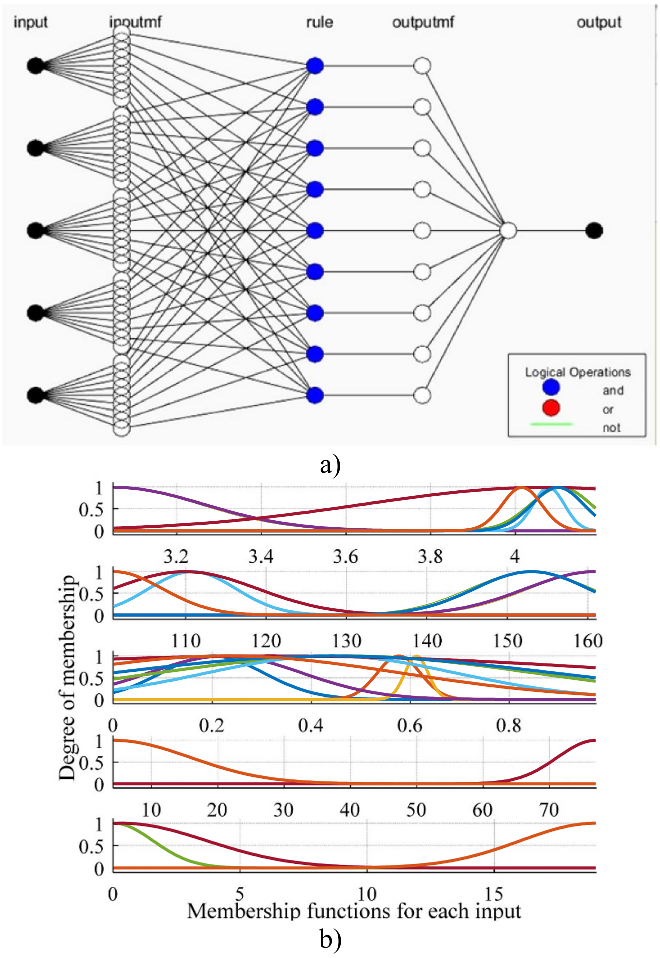

Figure 17. An investigation on the selected method for critical current estimation (a) the structure of layers in FCM9 ANFIS (b) membership functions of the FCM9 for each input.

6. Conclusion

The estimation of the critical current and the stress of the HTS tapes is a problem dealing with electromechanical considerations and thermomagnetic conditions. To solve such problem, finite element-based methods could be applied, however, they need a long time to compute the electromechanical characteristic of the HTS tapes. On the other hand, any action to reduce their computation time may compromise the accuracy. There are also other methods like equivalent circuit models or stochastic predictions. These methods are faster than FEMs with a lower accuracy.

Therefore, neither of these methods can be implemented in real-time which need a fast and highly accurate result. Thus, data-driven models based on AI techniques are becoming of interest which is due to their very high computational speed and high accuracy. This paper has proposed a model based on adaptive Neuro-fuzzy inference systems to estimate the electromechanical characteristic of twisted YBCO taps while the temperature, magnetic flux density, and strain are imposed as thermomagnetic conditions. The proposed method is a combination of fuzzy systems and neural networks. This causes higher computational speed and accuracy in comparison to other aforementioned methods. The impact of multiple membership functions and clustering methods were tested on the accuracy and the speed of estimation. The input data bank was established based on experimental tests of published papers reported in literature.

The most important findings of this paper are summarised as below:

- For the estimation of critical current, fuzzy clustering method with nine membership functions fulfils the accuracy and speed constraints while the most accurate method is sub-clustering method with clustering radius of 0.5 with R^2 and RMSE values of 0.047 and 0.92 and the fastest method is fuzzy clustering method with three membership functions and a computation time of 0.628 s.
- For the estimation of stress, fuzzy clustering method with three membership functions is the best approach considering both speed and accuracy constraints while the fastest method is sub-clustering method with clustering radius of 1 and estimation time 0.689 s.
- By applying the magnetic flux density out of the training range (i.e. data between 0–3 T) to the model, critical current was estimated accurately with an R^2 value of 0.72–0.957. It proves the effectiveness of the proposed ANFIS model for estimating data which it never saw before. This technically simulate the real-time condition.

It is worth noting that, the proposed model is still offline, however, in the future, it could be adjusted into a real-time method for estimating in an online manner. The only requirement for this is a high-performance computational system to bring the estimation time around couple of milliseconds.

Data availability statement

All data that support the findings of this study are included within the article (and any supplementary files).

ORCID iD

Mohammad Yazdani-Asrami https://orcid.org/0000-0002-7691-3485

References

[1] Ryu K S, Jo Y S and Park M 2006 Overview of the development of the advanced power system by the applied superconductivity technologies programme in Korea *Supercond. Sci. Technol.* **19** S102

[2] Yazdani-Asrami M, Asghar Gholamian S, Mirimani S M and Adabi J 2018 Calculation of AC magnetizing loss of ReBCO superconducting tapes subjected to applied distorted magnetic fields *J. Supercond. Novel Magn.* **31** 3875–88

[3] Sadeghi A, Seyyedbarzegar S M and Yazdani-Asrami M 2021 Transient analysis of a 22.9 kV/2 kA HTS cable under short circuit using equivalent circuit model considering different fault parameters *Physica* C **589** 1353935

[4] Sadeghi A and Seyyedbarzegar S M 2021 An accurate model of the high-temperature superconducting cable by using

stochastic methods *Transform. Mag.* **8** 24–30 (https://hrcak.srce.hr/263823)
[5] Ghabeli A, Yazdani-Asrami M, Besmi M R and Asghar Gholamian S 2015 Optimization of distributive ratios of apportioned winding configuration in HTS power transformers for hysteresis loss and leakage flux reduction *J. Supercond. Novel Magn.* **28** 3463–79
[6] Yazdani-Asrami M, Staines M, Sidorov G and Eicher A 2020 Heat transfer and recovery performance enhancement of metal and superconducting tapes under high current pulses for improving fault current-limiting behavior of HTS transformers *Supercond. Sci. Technol.* **33,** S095014
[7] Safaei. A, Zolfaghari M, Gilvanejad M and Gharehpetian G B 2020 A survey on fault current limiters: development and technical aspects *Int. J. Electr. Power Energy Syst.* **118** S105729
[8] Song W, Pei. X, Zeng X, Yazdani-Asrami M, Fang X, Fang J and Jiang Z 2020 AC losses in noninductive SFCL solenoidal coils wound by parallel conductors *IEEE Trans. Appl. Supercond.* **30** 1–9
[9] Yazdani-Asrami M, Zhang M and Yuan W 2021 Challenges for developing high temperature superconducting ring magnets for rotating electric machine applications in future electric aircrafts *J. Magn. Magn. Mater.* **522** 167543
[10] Kim J G, Salmani M A, Graber L, Kim H C and Pamidi S V 2015 Electrical characteristics and transient analysis of HTS DC power cables for shipboard application *IEEE Electric Ship Technologies Symp. (ESTS)* pp 376–81
[11] Yazdani-Asrami M, Song W, Pei X, Zhang M and Yuan W 2020 AC loss characterization of HTS pancake and solenoid coils carrying nonsinusoidal currents *IEEE Trans. Appl. Supercond.* **30** 1–9
[12] Shin H S, Dizon J R C, Kim T H, Ha D W and Oh S S 2007 Critical current degradation behavior in YBCO coated conductors under torsional strain *IEEE Trans. Appl. Supercond.* **17** 3274–7
[13] Majkic G, Mensah R J, Selvamanickam V, Xie Y Y and Salama K 2009 Electromechanical behavior of IBAD/MOCVD YBCO coated conductors subjected to torsion and tension loading *IEEE Trans. Appl. Supercond.* **19** 3003–8
[14] Takayasu M, Chiesa L, Bromberg L and Minervini J V 2010 Cabling method for high current conductors made of HTS tapes *IEEE Trans. Appl. Supercond.* **21** 2340–4
[15] Yazdani-Asrami M *et al* 2021 Artificial intelligence for superconducting transformers *Transformers Mag.* **8** 22–30 (https://hrcak.srce.hr/263818)
[16] Yazdani-Asrami. M, Gholamian S A, Mirimani S M and Adabi J 2019 Experimental investigation for power loss measurement of superconducting coils under harmonic supply current *Measurement* **132** 324–9
[17] Yazdani-Asrami M, Song W, Zhang M, Yuan W and Pei X 2021 Magnetization loss in HTS coated conductor exposed to harmonic external magnetic fields for superconducting rotating machine applications *IEEE Access* **9** 77930–7
[18] Staines M, Yazdani-Asrami M, Glasson N, Allpress N, Jolliffe L and Pardo E 2017 Cooling systems for HTS transformers: impact of cost, overload, and fault current performance expectations *Proc. 2nd Int. Workshop Cooling Syst. HTS Appl. (IWC-HTS)* (https://doi.org/10.5445/IR/1000075561)
[19] Ta W and Gao Y 2018 Numerical simulation of the electro-thermo-mechanical behaviors of a high-temperature superconducting cable *Compos. Struct.* **192** 616–25
[20] Seyyedbarzegrar S M and Mirzaie M 2015 ANFIS based model for power loss estimation of metal oxide surge arrester *J. Intell. Fuzzy Syst.* **29** 1779–86
[21] Zhao S, Blaabjerg F and Wang H 2021 An overview of artificial intelligence applications for power electronics *IEEE Trans. Power Electron.* **36** 4633–58
[22] Yazdani-Asrami M, Taghipour-Gorjikolaie M, Song W, Zhang M and Yuan W 2020 Prediction of nonsinusoidal AC loss of superconducting tapes using artificial intelligence-based models *IEEE Access* **8** 207287–97
[23] Michie D, Spiegelhalter D J and Taylor C C 1994 Machine learning, neural and statistical classification (https://doi.org/10.2307/1269742)
[24] Saadat S A, Fateh M M and Keighobadi J 2021 Adaptive state augmented clustering-based fuzzy learning control of a passive torque simulator *Int. J. Dyn. Control* 1–13
[25] Su. M C, Liu C W and Tsay S S 1999 Neural-network-based fuzzy model and its application to transient stability prediction in power systems *IEEE Trans. Syst. Man Cybern.* C **29** 149–57
[26] Chiu S L 1994 Fuzzy model identification based on cluster estimation *J. Intell. Fuzzy Syst.* **2** 267–78
[27] Saadat. S A, Ghamari S M, Mollaee H and Khavari F 2021 Adaptive neuro-fuzzy inference systems (ANFIS) controller design on single-phase full-bridge inverter with a cascade fractional-order PID voltage controller *IET Power Electron.* **14** 1960–72
[28] Pang M B and Zhao X P 2008 Traffic flow prediction of chaos time series by using subtractive clustering for fuzzy neural network modeling *Int. Symp. on Intelligent Information Technology Application* vol 1 pp 23–27
[29] Barth C, Mondonico G and Senatore C 2015 Electro-mechanical properties of REBCO coated conductors from various industrial manufacturers at 77 K, self-field and 4.2 K, 19 T *Supercond. Sci. Technol.* **28** S045011
[30] Shin H S, Dedicatoria M J, Awaji S and Watanabe K 2012 Characteristic strain response of I_C in SmBCO coated conductor tapes under magnetic field at 77 K *IEEE Trans. Appl. Supercond.* **22** 6600404
[31] Cheggour N, Ekin J W, Thieme C L H, Xie Y Y, Selvamanickam V and Feenstra R 2005 Reversible axial-strain effect in Y–Ba–Cu–O coated conductors *Supercond. Sci. Technol.* **18** S319
[32] Sugano M, Nakamura T, Manab T, Shikimachi K, Hirano N and Nagaya S 2008 The intrinsic strain effect on critical current under a magnetic field parallel to the *c* axis for a MOCVD-YBCO-coated conductor *Supercond. Sci. Technol.* **21** S115019
[33] Sugano M, Shikimachi K, Hirano N and Nagaya S 2010 The reversible strain effect on critical current over a wide range of temperatures and magnetic fields for YBCO coated conductors *Supercond. Sci. Technol.* **23** S085013
[34] Fleiter J, Sitko M and Ballarino A 2012 Analytical formulation of I_C dependence on torsion of YBCO and BSCCO conductors *IEEE Trans. Appl. Supercond.* **23** 8000204
[35] Shin H S and Dedicatoria M J 2012 Variation of the strain effect on the critical current due to external lamination in REBCO coated conductors *Supercond. Sci. Technol.* **25** S054013
[36] van der Laan D C, Ekin J W, Douglas J F, Clickner C C, Stauffer T C and Goodrich L F 2010 Effect of strain, magnetic field and field angle on the critical current density of $Y Ba_2Cu_3O_{7-\delta}$ coated conductors *Supercond. Sci. Technol.* **23** 072001
[37] Senatore C, Barth C, Bonura M, Kulich M and Mondonico G 2015 Field and temperature scaling of the critical current density in commercial REBCO coated conductors *Supercond. Sci. Technol.* **29** S014002
[38] Ma H, Liu H, Liu F, Zhang H, Ci L, Shi Y and Lei L 2018 Critical current measurements of high-temperature superconducting short samples at a wide range of temperatures and magnetic fields *Rev. Sci. Instrum.* **89** S015102